ELSEVIER

International Journal of Solids and Structures 41 (2004) 4551–4565

INTERNATIONAL JOURNAL OF SOLIDS and STRUCTURES

www.elsevier.com/locate/ijsolstr

Elastic solutions for periodically layered strip with perfect bonding or with an interface crack

Leonid Kucherov, Michael Ryvkin *

Department of Solid Mechanics, Materials and Systems, The Iby and Aladar Fleischman Faculty of Engineering, Tel Aviv University, 69978 Ramat Aviv, Israel

Received 14 September 2003; received in revised form 16 February 2004
Available online 9 April 2004

Abstract

A non-homogenization approach to the analysis of a strip consisting of a finite number of isotropic elastic layers arranged periodically is presented. The result is obtained by the use of the representative cell method based on the discrete Fourier transform. Two types of problems are addressed. In the problems of the first type the bonding between the layers is perfect. The solution for this case is found in a closed form in terms of the Laplace integrals. The numerical results for different boundary conditions are given and a comparison with plate theory is carried out. In the problems of the second type there is a flaw (crack) at one of the interfaces. The solution in this case hinges on the analytic expression for the Green function corresponding to a single interface dislocation in the uncracked strip. By using this expression the crack problem is reduced to a singular integral equation. The influence of the elastic mismatch and other problem parameters on the fracture characteristics is examined. It is found that, similar to the case of the periodic plane, when the thinner layeres in the strip are stiffer, further increase of their stiffness may lead to the increase or to the decrease of the absolute value of the stress intensity factor depending upon the elastic mismatch between the composite constituents.

Keywords: Periodically layered composite; Discrete Fourier transform; Interface crack

1. Introduction

Multilayered composite materials are widely used in modern engineering practice. Applications can be found in electronics, optics, aircraft and machining tool industries, and shipbuilding. The evaluation of the stress state in multilayers is a complicated task because of the stress discontinuity taking place at the multiple interfaces. Employing powerful numerical methods becomes less efficient with increase of the number of layers. Significant elastic and geometric mismatch between the composite constituents observed in many multilayers poses additional numerical problems. Consequently, some assumptions regarding through-thickness displacements distribution are usually made in the framework of the approximate plate theories. Another approach diminishing the computational cost is based on the hierarchy methods (e.g.

* Corresponding author.
E-mail address: arikr@eng.tau.ac.il (M. Ryvkin).

0020-7683/$ - see front matter © 2004 Elsevier Ltd. All rights reserved.
doi:10.1016/j.ijsolstr.2004.02.032

Babushka et al., 1992). A rather complete review of the state of art in the field of computational analysis of multilayered structures is given by Carrera and Demasi (2002).

Clearly, there is a need for verifying the approximate approaches by exact elasticity solutions. Such solutions for the simple supported 2D and 3D multilayers composed of anisotropic materials were obtained by Pagano (1969, 1970). The limitation of these solutions is that they are inconvenient to employ for the case of a large number of layers. A first goal of the present paper is to obtain the closed form exact solution free of the above limitation. For the specific case of periodically layered composites this can be done by means of the discrete Fourier transform based approach suggested by Nuller (1981). A similar method in the context of periodic structures was developed by Karpov et al. (2002).

The knowledge of the stress distribution in perfectly bonded multilayers provides the ground for the fracture analysis. One of the most commonly encountered fracture modes is the interface delamination. In most studies of this phenomenon either composites with a limited number of layers are considered (e.g. Chatterjee, 1987; Schoeppner and Pagano, 1998; Bruno and Greco, 2001) or some homogenization procedure is exploited (Sheinman and Kardomates, 1997). Several works are dedicated to periodically layered composites. Charalambides (1991) used laminate theory in the analysis of a cross-ply laminated beam. Kaczyński et al. (1994) solved the problem on an interface crack in a periodically layered strip by a non-standard homogenization technique. However, we will show that the discrete Fourier transform based general approach works as well in the presence of the interface crack, and it is possible to obtain the solution without simplifying assumptions. The second goal of the present study is to obtain such a solution. As in the case of an interface crack in a periodically layered bi-material plane including an infinite number of layers (Kucherov and Ryvkin, 2002) the initial problem is reduced to a singular integral equation.

In the next section the exact elastic solution for the perfectly bonded periodically layered bi-material infinite strip is derived. The solution is expressed in quadratures. It is implemented for two different types of boundary conditions at the strip edges. The numerical results are presented, and a parametric study is performed. In Section 3 a strip containing an interface delamination crack is considered. In accordance with the dislocation method (Erdogan and Gupta, 1971a,b) the crack is viewed as a superposition of point dislocations. The Green function for a single dislocation is determined in a closed form by the technique developed in Section 2. This enabled to formulate a singular integral equation from which the stress intensity factor and the energy release rate were determined. The results are verified by comparison with known solutions from the literature for the limiting cases. The final section presents the concluding remarks.

2. Periodically layered bimaterial strip with perfect bonding

2.1. Closed form solution

Consider an infinite composite bimaterial strip Ω of thickness H. The strip consists of perfectly bonded isotropic elastic layers of two different types arranged periodically (Fig. 1a). The thickness, shear modulus and Poisson ratio of the layers of rth type are denoted as h_r, μ_r and ν_r, respectively $(r = 1, 2)$. A method of deriving the stress state in such strip under arbitrary boundary conditions on its edges has been suggested by Nuller (1981). This method which is implemented below, hinges on the representative cell approach (Nuller and Ryvkin, 1980; Ryvkin and Nuller, 1997) and enables to obtain a closed form analytical solution of the problem. Suppose, for definiteness, that the total number of layers is even, then the strip may be viewed as an assemblage of bonded identical cells $\Omega_k, k = 0, \ldots, N-1$ of thickness $h = h_1 + h_2$ (the case of a strip with an odd number of layers can be also addressed without difficulty). The typical cell Ω_k consisting of two dissimilar layers is depicted in Fig. 1b. In accordance with the representative cell approach, systems of local coordinates x,y are introduced in all cells in an identical manner as shown in the figure. It is convenient to introduce a vector related to the stress–strain state in the rth layer of the kth cell as follows

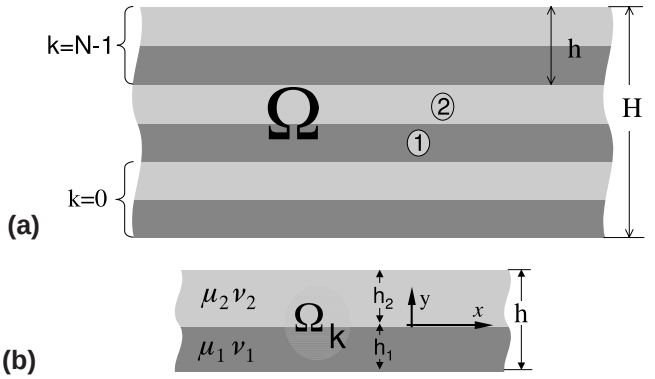

Fig. 1. Periodically layered bi-material strip (a) and its repetitive cell (b).

$$\boldsymbol{U}_r^{(k)}(x,y) = \{u_r^k, v_r^k, \sigma_r^k, \tau_r^k\}, \tag{1}$$

where $u_r^k \equiv u_r^k(x,y)$ and $v_r^k \equiv v_r^k(x,y)$ are the displacements in the x- and y-directions, respectively, and $\sigma_r^k \equiv \sigma_r^k(x,y)$ and $\tau_r^k \equiv \tau_r^k(x,y)$ are the normal and shear stresses acting at the planes parallel to the interfaces. Then the boundary value problem for the strip in the case of the prescribed tractions at its edges is defined by the following system of equations (the adopted cells numbering is upwards from the bottom)

$$L_r[u_r^k(x,y), v_r^k(x,y)] = 0, \quad k = 0,\ldots,N-1 \quad r = 1,2, \tag{2}$$

$$\boldsymbol{U}_2^k(x,0) - \boldsymbol{U}_1^k(x,0) = 0, \quad k = 0,\ldots,N-1, \tag{3}$$

$$\boldsymbol{U}_1^k(x,-h_1) - \boldsymbol{U}_2^{k-1}(x,h_2) = 0, \quad k = 1,\ldots,N-1, \tag{4}$$

$$\sigma_2^{N-1}(x,h_2) = \sigma^u(x), \tag{5}$$

$$\tau_2^{N-1}(x,h_2) = \tau^u(x), \tag{6}$$

$$\sigma_1^0(x,-h_1) = \sigma^b(x), \tag{7}$$

$$\tau_1^0(x,-h_1) = \tau^b(x). \tag{8}$$

Here operator L_r in Eqs. (2) corresponds to the Lamé field equations, and the next group of equations define the bonding conditions at the interfaces within the cells (3) and between the neighboring cells (4). Eqs. (5)–(8) express the stress boundary conditions at the upper and bottom edges of the strip, where the given tractions are denoted by the superscripts (u) and (b), respectively.

The considered domain in spite of its periodic structure does not possess the translational symmetry in the direction perpendicular to the interfaces. Consequently, the representative cell technique based on the discrete Fourier transform can not be applied directly. To overcome this obstacle we complete the strip to a plane by adding infnite number of cells Ω_k, $k = \ldots,-2,-1,N,N+1,\ldots$ and suppose that the stress state in the plane possesses the periodicity property with period equal to hP, where P is some integer grater than N. In terms of local coordinates this property is expressed as following

$$\boldsymbol{U}_r^{k+nP}(x,y) = \boldsymbol{U}_r^k(x,y), \quad r = 1,2; \quad k = 1,\ldots,P-1, \quad n = 0,\pm1,\pm2\ldots, \tag{9}$$

i.e. the plane consists of P-strips with identical stress state.

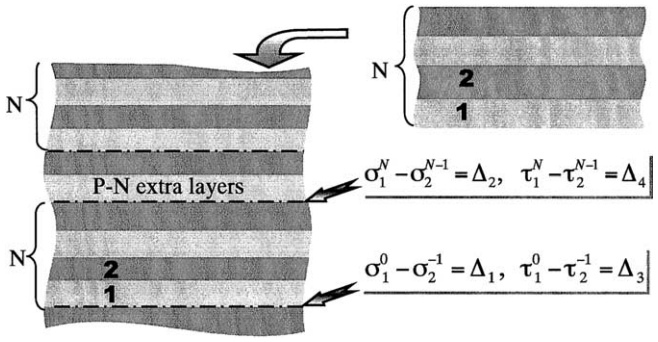

Fig. 2. Transition from the problem for a strip to the problem for a plane.

Each P-strip, in turn, may be viewed as composed of the initial N-strip and $P-N$ additional cells (Fig. 2). The above condition, clearly, will take place only if the loading applied to the plane is P-periodic. In order to keep the equivalence to the initial problem we assume that this loading is applied in the region occupied by $P-N$ additional cells. It is convenient to apply the loading at the interfaces corresponding to the bottom and the upper edges of the initial strip (Fig. 2). Consequently, the equilibrium conditions at these interfaces take the form

$$\begin{aligned}
&\sigma_1^{nP}(x,-h_1) - \sigma_2^{nP-1}(x,h_2) = \Delta_1(x),\\
&\tau_1^{nP}(x,-h_1) - \tau_2^{nP-1}(x,h_2) = \Delta_3(x),\\
&\sigma_1^{N+nP}(x,-h_1) - \sigma_2^{N-1+nP}(x,h_2) = \Delta_2(x),\\
&\tau_1^{N+nP}(x,-h_1) - \tau_2^{N-1+nP}(x,h_2) = \Delta_4(x), \quad n = 0,\pm1,\pm2\ldots.
\end{aligned} \tag{10}$$

The unknown stress jumps Δ_i are to be adjusted in order to provide the fulfillment of conditions (5)–(8) at the boundaries of the N- strip. Their derivation is carried out by taking advantage of the cyclic symmetry of the stress state in the plane. A similar technique for replacing the problem for an arbitrary loaded finite periodic structure by the equivalent cyclic one was employed recently by Karpov et al. (2002). Note that there is some freedom in choosing the location of the jumps as well as their origin. For example, jumps in the displacements can be considered. The interested reader can find more information on this subject in the paper by Nuller (1981).

Let us cut out from the plane one cycle, a P-strip comprised of the cells Ω_k, $k = 0,1,\ldots,P-1$. The boundary problem for this strip is defined by the field equations (2), the conditions at the inner interfaces (3) and the conditions between the cells

$$\boldsymbol{U}_1^k(x,-h_1) - \boldsymbol{U}_2^{k-1}(x,h_2) = \boldsymbol{D}^0(x)\delta_{k0} + \boldsymbol{D}^N(x)\delta_{kN} \tag{11}$$

completed by the periodicity condition following from (9)

$$\boldsymbol{U}_2^P(x,-h_1) = \boldsymbol{U}_r^0(x,-h_1). \tag{12}$$

Here the vectors $\boldsymbol{D}^d(x) = \{0,0,\Delta_1(x),\Delta_3(x)\}$ and $\boldsymbol{D}^u(x) = \{0,0,\Delta_2(x),\Delta_4(x)\}$ are composed from the introduced stress jumps and δ_{ij} is the Kronecker delta.

Application of the finite discrete Fourier transform

$$g_r^*(x,y,\phi_m) = \sum_{k=0}^{P-1} g_r^k(x,y)\mathrm{e}^{-\mathrm{i}k\phi_m}, \quad \varphi_m = 2\pi m/P, \quad m = 0,1,2,\ldots,P-1 \tag{13}$$

reduces the problem for the P-strip to the boundary problem for the representative cell Ω^* ($-h_1 < y < h_2$, $-\infty < x < \infty$)

$$L_r[u_r^*(x,y,\varphi_m), v_r^*(x,y,\varphi_m)] = 0, \quad (x,y) \in \Omega^*, \tag{14}$$

$$\boldsymbol{U}_2^*(x,0,\varphi_m) - \boldsymbol{U}_1^*(x,0,\varphi_m) = 0, \tag{15}$$

$$\boldsymbol{U}_1^*(x,-h_1,\varphi_m) - \gamma_m \boldsymbol{U}_2^*(x,h_2,\varphi_m) = \boldsymbol{D}^d(x) + \boldsymbol{D}^u(x)\gamma_m^N, \tag{16}$$

where $\gamma_m = \mathrm{e}^{-\mathrm{i}\varphi_m}$.

Note that conditions (16) relating the opposite sides of the representative cell are sometimes referred as Born–Von Karman type boundary conditions.

The solution of the problem for the representative cell is straightforward. The Papkovich-Neuber representation of the displacements transforms in the form of Laplace integrals

$$\begin{aligned}
u_r^*(x,y,\varphi_m) &= \frac{1}{2\pi}\int_L [yz(A_{4r-1}\cos zy + A_{4r}\sin zy) + A_{4r-3}\cos zy + A_{4r-2}\sin zy]\mathrm{e}^{zx}\,\mathrm{d}z,\\
v_r^*(x,y,\varphi_m) &= \frac{1}{2\pi}\int_L [(A_{4r-2} - (3-4\nu_r)A_{4r-1} + yzA_{4r})\cos zy - (yzA_{4r-1} + \kappa_r A_{4r} + A_{4r-3})\sin zy]\mathrm{e}^{zx}\,\mathrm{d}z,\\
\kappa_r &= 3 - 4\nu_r; \quad r = 1,2
\end{aligned} \tag{17}$$

provides the fulfillment of field equations (14). Here $A_j \equiv A_j(z)$, $j = 1,2,\ldots,8$ are the functions of complex variable z, and contour L is a line $\mathrm{Re}\, z = \varepsilon$ in the z-plane. The exact location of the contour L in the vicinity of the imaginary axis must be chosen in accordance with the boundary conditions in order to provide the required behavior of the solution for $x \to \infty$.

Substitution of (17) into the boundary conditions (15) and (16) yields after some manipulation the system of 8 linear algebraic equations with respect to unknown functions A_j

$$\boldsymbol{M}\boldsymbol{A} = \boldsymbol{R}. \tag{18}$$

Here $\boldsymbol{A} = \{A_j\}$, $\boldsymbol{R} = \{0;0;\bar{A}_1(z) + \gamma_m^N \bar{A}_2(z);\bar{A}_3(z) + \gamma_m^N \bar{A}_4(z);0;0;0;0\}$, and the square matrix $\boldsymbol{M} = \{m_{ij}\}$ is presented in Appendix A. The upper bar denotes hereafter the Laplace transforms of the corresponding functions.

Having defined functions A_j in terms of the unknown jumps one can determine the components of the stress–strain state in any cell Ω_k, $k = 0,1,2,\ldots,P-1$ of the P-strip by the inverse discrete Fourier transform

$$g_r^k(x,y) = \frac{1}{P}\sum_{m=0}^{P-1} g_r^*(x,y,\phi_m)\mathrm{e}^{\mathrm{i}k\varphi_m}. \tag{19}$$

The jumps are determined from conditions (5)–(8) which provide the equivalence of the P-strip and N-strip problems within domain Ω. The 4th order linear algebraic system for deriving the Laplace transforms of the jumps has the form

$$\left(\frac{1}{P}\sum_{m=0}^{P-1}\begin{bmatrix} s_{11} & \gamma_m^N s_{11} & s_{13} & \gamma_m^N s_{13}\\ s_{21} & \gamma_m^N s_{21} & s_{23} & \gamma_m^N s_{23}\\ \gamma_m^{-N} s_{11} & s_{11}-1 & \gamma_m^{-N} s_{13} & s_{13}\\ \gamma_m^{-N} s_{21} & s_{21} & \gamma_m^{-N} s_{23} & s_{23}-1 \end{bmatrix}\right)\begin{bmatrix} \bar{\Delta}_1(z)\\ \bar{\Delta}_2(z)\\ \bar{\Delta}_3(z)\\ \bar{\Delta}_4(z)\end{bmatrix} = \begin{bmatrix} \bar{\sigma}^d(z)\\ \bar{\tau}^d(z)\\ \bar{\sigma}^u(z)\\ \bar{\tau}^u(z)\end{bmatrix}, \tag{20}$$

where the expressions for the elements s_{ij} are given in Appendix B. These expressions depend upon discrete Fourier transform parameter m, and the summation is understood as being applied to any element of the matrix. Having derived the jumps transforms from the latter system one obtains in view of (17)–(19) the closed form solution of the initial problem (2)–(8) on the periodically layered bi-matetrial strip Ω.

Exchanging the order of the summation and the integration gives the answer in the form of Laplace integrals of rather cumbersome expressions which can be, nevertheless, successfully handled using symbolic computation. It should be noted that when the external loading at the strip edges is localized and the stresses at infinity vanish the Laplace transforms of the stresses do not possess singularities on the imaginary axis and contour L can be shifted to the line $\mathrm{Re}\, z = 0$, which facilitates the calculation procedure.

Note, that the number $P - N$ of additional cells in the P-strip can be chosen arbitrarily and, of course, does not influence the final result. It was found that it is most convenient to take the thickness of the P-strip about 5% larger than that of the N-strip. Another point that should be emphasized is that with increasing number of bilayers N and, consequently, of P, defining the number of terms in (19), the numerical efficiency of the method decreases. This phenomenon can be cancelled out by setting $P \to \infty$ and replacing the finite discrete Fourier transform by the discrete Fourier transform. The interested reader can find the detailed description of this procedure in Kamysheva et al. (1982).

2.2. Numerical examples

Let us first compare the obtained exact solution with the approximate theory of composite plates by means of the three point bending specimen (see insert in Fig. 3b). An infinite strip consisting of twenty bilayers ($N = H/h = 20$) is subjected to a normal point force Q applied between the simple supports in a non-symmetric manner $l_1/H = 1$, $l_2/H = 4$. The thinner layers are assumed to be the more compliant ones $h_1/h = 0.2$, $\mu = \mu_2/\mu_1 = 20$ and the Poisson ratios of the materials are taken as $\nu_1 = 0.3$ and $\nu_2 = 0.35$.

The external tractions in boundary conditions at the strip edges (5)–(8) are found to be

$$\sigma^u(x) = -Q\delta(x - l_1), \tag{21}$$

$$\sigma^b(x) = -Q\left[\frac{l_2}{l}\delta(x) + \frac{l_1}{l}\delta(x - l)\right], \tag{22}$$

$$\tau^u(x) = \tau^b(x) = 0, \tag{23}$$

where $\delta(x)$ is the delta function and $l = l_1 + l_2$ is the distance between the supports.

The numerical results for the stress distribution are presented in the global Cartesian coordinate system (X, Y). In Fig. 3a and b the normalized bending stresses $\sigma_{xx}(X_0, Y)$ composed from the corresponding values $\sigma^k_{r_{xx}}(x, y)$ are shown.

Two cross-sections $X_0/H = 3$ and $X_0/H = 1$ are considered. Both graphs are discontinuous at the interfaces between the layers because of the jumps in the elastic properties. For the cross-section away from the point forces (Fig. 3a) the stresses within each layer exhibit linear behavior and parts of the graph corresponding to the stiff and the compliant layers are located along the two different straight lines. Such a behavior points to a linear bending strain distribution in the N-strip which is in agreement with the plane cross-sections hypothesis adopted in the plate theory of composites. In fact, the stresses calculated by the use of this theory (dotted line) are found to be very close to the exact values.

On the other hand, in the cross-section where the point force is applied the plate theory, as expected, does not give satisfactory results (Fig. 3b). The stress distribution within each of the layers is found to be linear as in the previous case. This may be explained by a relatively large difference in the elastic moduli of the materials, when the thick stiff layers behave like beams and the thin compliant ones like linear springs.

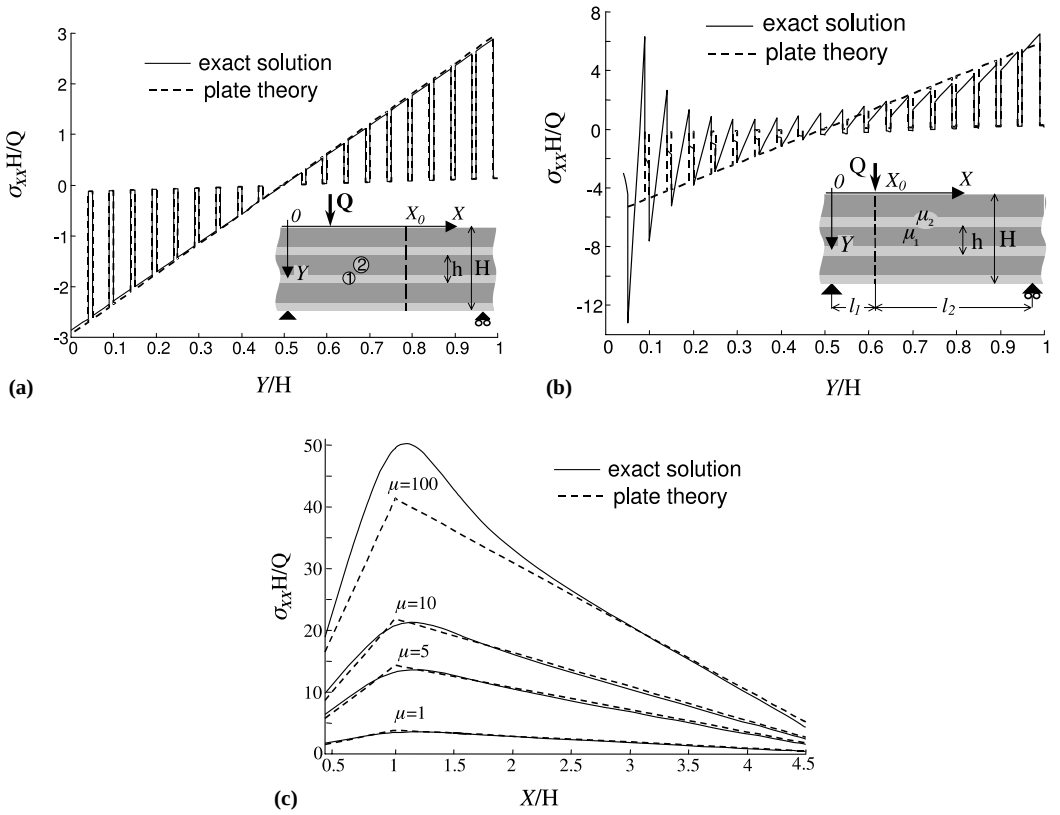

Fig. 3. Bending stress in the three point bending problem in the cross-section away from the point forces (a), in the cross-section including the applied force (b) and within the stiffer layer along the interface closest to the bottom edge (c).

At the same time, the angles defining the linear distribution within the layers of the specific type are different and the bending strain is a non-linear function of through-thickness coordinate Y.

Another comparison of the obtained solution with the plate theory is presented in Fig. 3c where the distribution of the bending stress $\sigma_{xx}(X, H - h_1 - 0)$ along the first interface from the bottom is depicted. The results are presented for different materials mismatch. It is seen that for the considered geometry the difference between the plate theory and the exact solution becomes significant only for large elastic moduli ratio and decreases rapidly with the distance from the cross-section where the point force is applied.

In the next example the contact stresses at the interface between the multilayered strip and the rigid substrate are examined (see insert in Fig. 4a). The loading is a tangential shear force applied at the upper edge. The bonding between the strip and the substrate is perfect and the stress boundary conditions (7) and (8) are to be replaced by the clamping conditions

$$u_1^0(x, -h_1) = v_1^0(x, -h_1) = 0. \tag{24}$$

The change in the type of boundary conditions does not preclude employing, as previously, the stress jumps Δ_j as the adjusting factor. The matrix equation (18) remains unaltered. When correcting the first two equations of (20) in accordance with (24) one obtains the closed form solution in this case also.

The calculations were carried out for the strip consisting of eight bi-layers. The materials of the composite constituents have dissimilar shear moduli $\mu = \mu_2/\mu_1 = 9$ and equal Poisson ratios $\nu_1 = \nu_2 = 1/3$. The

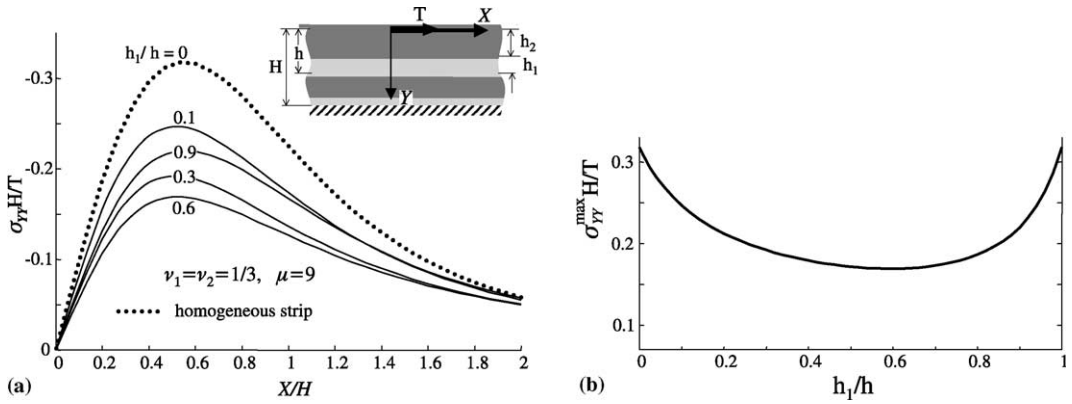

Fig. 4. (a) Normal contact stresses at the interface between the strip and rigid substrate. (b) Dependence of the maximal normal contact stress upon the volume fraction of the first material.

numerical results for the normal contact stresses at the strip bottom $Y = H$ for different thickness ratios h_1/h are presented in Fig. 4a. The stresses are screw symmetric and are shown for $X > 0$. It is worthwhile to compare the obtained results with the solution of the corresponding problem on a homogeneous strip. The stresses in the analytical solution of the latter problem, which is easily derived by the standard Laplace transformation technique (see, for example, Uflyand, 1968), are found to be independent of the material shear modulus. Consequently, the stress distribution for both limiting cases $h_1/h \to 0$ and $h_1/h \to 1$ in the considered problem on the multilayered strip must be the same. This trend is clearly observed in the figure where the analytical result for the homogeneous strip is denoted by a dotted line. Note, that in the case of materials with dissimilar Poisson ratios one would get two different limiting curves.

The stress distribution is characterized by a single maximum depending upon the volume fraction h_1/h. The results reveal an interesting phenomenon: for sufficiently thin layers of one type this maximum always decreases with the increasing of their thickness independently of the fact whether these layers are the stiffer or the more compliant ones. Consequently, the contact stresses at the bottom of the layered strip will, as a rule, be less than those for the strip made of the thick layers bulk material. Clearly, there is some optimum value of ratio h_1/h minimizing the maximum of the contact stresses. For the considered materials it is found to be about 0.6 as illustrated in Fig. 4b where the dependence of the maximum normal stress upon the thickness ratio is presented.

The calculations show that a similar phenomenon takes place in the conjugate problem when the shear stresses at the clamped bottom of the strip generated by a normal force applied at the upper edge are examined. Namely, there is some optimal thickness ratio minimizing the contact shear stresses.

3. Delamination crack

3.1. Singular integral equation

The extension of the employed method to the case when the bonding of the layers is not perfect and there is a crack at one of the interfaces is not a particulary diffficult problem. The change in the type of the boundary conditions at the cracked interface can be eliminated by using the dislocation approach suggested by Erdogan and Gupta (1971a,b). Recently this approach was successfully employed in combination with

the representative cell method for the problems about cracks in periodically layered composites (see references in Kucherov and Ryvkin (2002)).

Consider the case when a crack of length $2a$ is loaded by uniform opening tractions σ_0 and located at the inner interface in cell number n

$$\sigma_1^n(x,0) = \sigma_2^n(x,0) = -\sigma_0, \tag{25}$$

$$\tau_1^n(x,0) = \tau_2^n(x,0) = 0, \quad -a < x < a. \tag{26}$$

The upper edge of the strip is traction-free

$$\sigma_2^{N-1}(x,h_2) = \tau_2^{N-1}(x,h_2) = 0, \tag{27}$$

and the lower one is clamped, i.e. condition (24) takes place (see insert in Fig. 5). The reduction of the initial problem for a crack to a singular integral equation hinges on deriving the Green function for a single dislocation in the uncracked body. The corresponding boundary problem is defined by Eqs. (2), (4), (24) and (27) and a new bonding condition instead of (3)

$$\boldsymbol{V}_2^k(x,0) - \boldsymbol{V}_1^k(x,0) = \boldsymbol{F}(t)\delta(x-t)\delta_{kn}, \quad k = 0,\ldots,N-1, \tag{28}$$

where

$$\boldsymbol{V}_r^k(x,y) = \left\{ \frac{\partial u_r^k}{\partial x}, \frac{\partial v_r^k}{\partial x}, \sigma_r^0, \tau_r^0 \right\} \tag{29}$$

is the vector including the displacements derivatives in x-direction, vector $F(t) = \{f_1(t), f_2(t), 0, 0\}$ defines the jumps in these derivatives across the non-perfect interface with the dislocation at point $x = t$.

Since the dislocation in fact represents an additional loading and enters only the right hand side of the bonding conditions, the further steps in the solution are the same as in the previous section. Application of the finite discrete Fourier transform to the problem for the P-strip with the cyclic stress state leads to the boundary problem for the representative bi-layered cell defined by Eqs. (14), (16) and by the condition

$$\boldsymbol{V}_2^*(x,0,\varphi_m) - \boldsymbol{V}_1^*(x,0,\varphi_m) = \boldsymbol{F}(t)\delta(x-t)\gamma_m^n \tag{30}$$

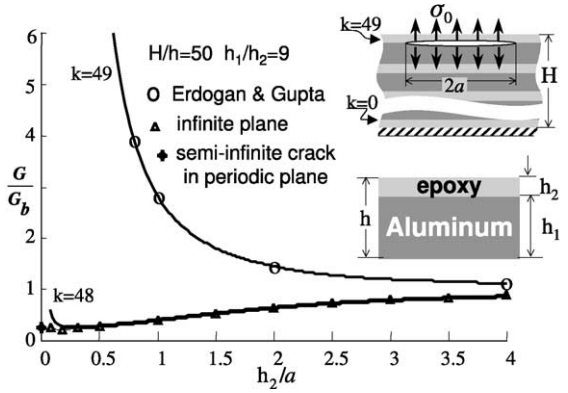

Fig. 5. Energy release rate for the uniformly loaded interface crack located at the first interface below the free edge (upper curve) and at the third one (lower curve).

at the interface. The solution of this problem is sought in the form of Laplace integrals (17), and the expressions for the eight functions A_j in terms of the four unknown jumps are derived from the boundary conditions (16) and (30)

$$A_j = \{M_{3j}[\bar{\Delta}_1(z) + \gamma_m^N \bar{\Delta}_2(z)] + M_{4j}[\bar{\Delta}_3(z) + \gamma_m^N \bar{\Delta}_4(z)] + \gamma_m^n \mathrm{e}^{-zt}[M_{5j} f_1(t) + M_{6j} f_2(t)]\} \Delta^{-1}, \quad j = 1, 2, \ldots, 8. \tag{31}$$

Here Δ is the determinant of matrix $\boldsymbol{M}$ from (18) and M_{ij} are the corresponding cofactors. The jumps are found from the 4th order system similar to (20) obtained by the use of homogeneous conditions (27) and (24) at the strip edges. Hence, in view of (17) and (19), the analytical expression of the Green function for the single interface dislocation is determined. This result is of importance since it allows to formulate different interface crack problems for a bi-material periodically layered strip in terms of singular integral equations. In the considered case of a single crack subjected to the loading defined in (25) and (26), the general procedure developed by Erdogan and Gupta (1971a,b) leads after some manipulation to the following equation

$$\frac{1}{\pi \mathrm{i}} \int_{-a}^{a} \frac{f(t)\,\mathrm{d}t}{t - x} - \beta f(x) + \int_{-a}^{a} [f(t) K_1(t, x)\,\mathrm{d}t + \bar{f}(t) K_2(t, x)]\,\mathrm{d}t = p, \tag{32}$$

where $f(t) = f_1(t) + \mathrm{i} f_2(t)$ is a complex dislocation, $\overline{f(t)}$ denotes the complex conjugate,

$$p = \frac{\mathrm{i}(\mu_1 - \mu_2)(1 - \beta^2)}{2\mu_1 \mu_2 (\alpha - \beta)} \sigma_0, \tag{33}$$

and α, β are the Dundurs elastic mismatch parameters

$$\alpha = \frac{\mu(\kappa_1 + 1) - (\kappa_2 + 1)}{\mu(\kappa_1 + 1) + (\kappa_2 + 1)}, \quad \beta = \frac{\mu(\kappa_1 - 1) - (\kappa_2 - 1)}{\mu(\kappa_1 + 1) + (\kappa_2 + 1)}. \tag{34}$$

The kernels of the equation are represented by the inverse Laplace and Fourier transforms

$$K_l(t, x) = \int_{-\infty}^{\infty} \mathrm{e}^{\mathrm{i}\xi(x - t)} \frac{1}{P} \sum_{m=0}^{P-1} \gamma_m^{-n} k_l(t, x)\,\mathrm{d}\xi, \quad l = 1, 2, \tag{35}$$

where functions $k_l(t, x)$ have lengthy expressions and are not exhibited for the sake of brevity.

The complex equation (32) represents a system of two scalar singular integral equations. Its solution by the use of Jacobi orthogonal polynomials and the ensuing derivation of the fracture characteristics is carried out following Erdogan and Gupta (1971b). The numerical results for the specific problems including the parametric study are presented in the following subsection.

3.2. Numerical results

The singular stress field at the interface ahead of the crack tip is expressed by means of the complex stress intensity factor K

$$\sigma_{yy}(x, 0) + \mathrm{i}\tau_{xy}(x, 0) = \frac{K}{\sqrt{2\pi(x - a)}} (x - a)^{\mathrm{i}\varepsilon}, \quad \varepsilon = \frac{1}{2\pi} \ln \frac{1 - \beta}{1 + \beta}. \tag{36}$$

Its absolute value together with the elastic parameters defines the energy release rate G (Malishev and Salganik, 1965)

$$G = \frac{|K|^2}{16} (1 - \beta^2) \left(\frac{\kappa_1 + 1}{\mu_1} + \frac{\kappa_2 + 1}{\mu_2} \right). \tag{37}$$

The normalized quantity $\hat{G}$, below, is obtained by the use of the energy release in the corresponding problem of a crack at the interface between two layers of infinite thickness, i.e., dissimilar half planes (Rice and Sih, 1965)

$$\hat{G} = \frac{G}{G_b} = \frac{|K|^2}{\pi a \sigma_0^2 (1 + 4\varepsilon^2)}. \tag{38}$$

The parameters of the multilayered strip in the first example are chosen in order to compare the results obtained by the proposed method with the ones known from the literature for some limiting cases. An aluminum/epoxy composite with thick aluminum layers ($h_1/h_2 = 9$) is examined. The materials properties are taken as following: for aluminum (material 1) $\mu_1 = 26.5$ GPa, $\nu_1 = 0.3$ and for epoxy (material 2) $\mu_2 = 11.5$ GPa, $\nu_2 = 0.35$. The total number of bi-layers $N = H/h$ is 50.

The dependence of the normalized energy release rate upon the relative crack length is presented in Fig. 5. The upper curve corresponds to the interface separated from the free upper edge by a single epoxy layer. Hence, the number of the cell with the imperfect interface n is 49. It is seen that increase of the crack length leads to the monotonic unlimited increase of the energy release. Since the underlying aluminum layer is significantly thicker and stiffer than the epoxy one, the results, as expected, meet the data obtained by Erdogan and Gupta (1971b) in the problem on a crack at the interface between the epoxy layer and the aluminum half plane. On the other hand, for the crack located at the third interface when $n = 48$ the observed behavior is vastly different. The energy release rate is found to be almost the same as in the problem on the crack in the periodically layered plane (Kucherov and Ryvkin, 2002). The influence of the free boundary emerges only when the crack length exceeds some critical value and the energy release rate increases rapidly.

In the following examples the cracked strip is loaded by two self-equilibrated point forces applied at the traction free boundaries (see insert in Fig. 6). In this case the integral equation is formulated by the use of the Green function for a single dislocation in a strip with free edges. Its derivation is carried out in the same manner as in the previous case of clamped-free boundary conditions.

In the first configuration the crack is located at the interface closest to the upper edge of the strip consisting of 50 symmetric bi-layers with $h_1 = h_2$. The absolute value of the stress intensity factor is examined. Its dependence upon the crack length for different material combinations with $\beta = 0$ and various shear moduli ratio $\mu = \mu_2/\mu_1$ is depicted in Fig. 6. The general behavior is similar to the one observed previously in the case of a uniformly loaded crack near the free edge. The rapid increase of the stress intensity factor with the increase of the crack length indicates beam-like behavior of the upper layer separated from the strip. In fact, the beam asymptotic (dashed line) derived for the specific case of a

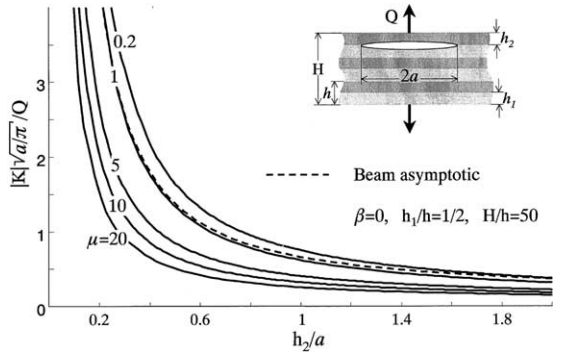

Fig. 6. Absolute value of the stress intensity factor vs. the crack length for different shear moduli ratio.

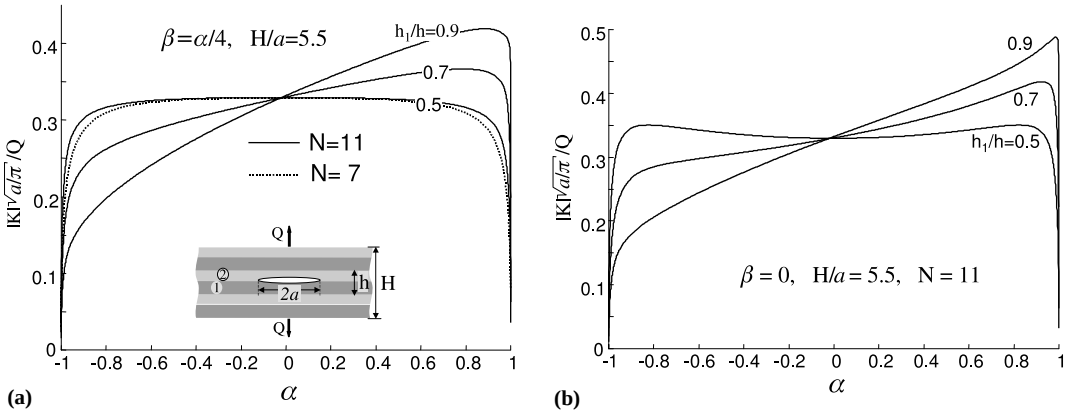

Fig. 7. Absolute value of the stress intensity factor vs. elastic mismatch parameter α for the cases $\beta = \alpha/4$ (a) and $\beta = 0$ (b).

homogeneous strip by Dyskin et al. (2000) approaches the corresponding curve $\mu = 1$ for sufficiently long cracks. The increase of the upper layer stiffness leads to monotonic decreasing of the stress intensity factor. Note that when the crack is located deeper inside the strip and the thicknesses of the layers, contrary to the considered case are not equal, the influence of the elastic mismatch on the stress intensity factor may be more complicated. This issue is illustrated below.

In the problem presented in Fig. 7a the crack is placed in the midline of the strip. The dependence of the stress intensity factor upon the elastic mismatch parameter α for the case $\beta = \alpha/4$ is exhibited. Consequently, $\alpha = 0$ corresponds to the case of identical materials, i.e., to the case of a homogeneous strip. The solid lines are related to the strip with 11 bi-layers and $h/a = 0.5$. For all the curves the thickness of the layers of the first type is equal or more than that of the second type. So, the increasing of α from zero for the curves with $h_1/h = 0.7,0.9$ may be understood as further increasing of the stiffness of the stiff thinner layers. It is seen that similar to the case of the crack in a periodically layered plane (Ryvkin and Kucherov, 2001) the above increasing may lead to the increase as well as to the decrease of the stress intensity factor. Therefore, for some material combination, it approaches a maximum value. Only in the particular case of equal thicknesses of the layers $h_1/h = 0.5$ the increasing of the elastic mismatch always leads to the decrease of the stress intensity factor. Hence, only in this case the absolute value of the stress intensity factor for the interface crack is less than the stress intensity factor for the crack in a homogeneous strip. Note that for the case $\beta = 0$ the observed phenomenon does not hold as can be seen in Fig. 7b. Therefore, generalizing the conclusions regarding interface fracture based on the relatively simple case $\beta = 0$ must be done very carefully. It is of interest to elucidate the influence of the scale parameter h/a on the stress intensity factor. This may be done by comparing two composites with the same volume fraction defined by the ratio h_2/h_1 and different thicknesses h of the repetitive cell. To this end the calculations for the strip with the diminished number of bi-layers ($N = 7$, $h/a = 0.786$) have been carried out. The results presented in Fig. 7a by the dotted line show that for any elastic mismatch the stress intensity factor is weakly affected by the change in the layering scale h/a.

As it is well known, the mathematical solution of the interface crack problem with the conditions of the type (25) and (26) on the crack line is characterized by the oscillating singularity (36). On the other hand the size r_c of the physically senseless interpenetration zone which can be derived following Rice (1988) may be large only in the specific cases with a significant amount of Mode II deformation. In both problem considered in this section the loading is normal to the crack line. Consequently, the calculations show, as expected, that the ratio r_c/a is negligibly small.

4. Concluding remarks

The method of analysis of periodically layered composite strips based on the discrete Fourier transform is implemented and found to be a convenient tool providing accurate results for both cracked and uncracked composites. In contrast to the known numerical methods the suggested approach is insensitive to the number of layers and to the geometric and elastic mismatch between the composite constituents. Rather cumbersome analytic expressions appearing during the solution procedure are successfully manipulated by the use of symbolic computation.

Several specific problems have been solved. The analysis of a periodically layered composite strip subjected to three point bending has shown, as expected, that in the vicinity of the point forces the cross-section of the strip does not remain plane after the deformation and, consequently, the approximate plate theory is not valid. On the other hand, it appeared that in the case of a large elastic mismatch between the materials the strain distribution in each individual layer is linear. The investigation of the protective properties of a periodically layered strip bonded to a substrate indicates that there is an optimal ratio between the layers thicknesses providing the minimum of the normal (shear) contact stresses resulting from the shear (normal) external loading.

In the study of cracked composites with an interface delamination crack two types of behavior have been observed. When the crack is near the strip edge the separated layer acts like a beam and the stress intensity factor can be found from the beam asymptotics. Alternatively, when the crack is located not too close to the strip boundary the behavior typical for the crack in a periodically layered plane emerges. It was found that, similar to the case of a crack in a periodically layered plane, if the thinner layers in the strip are the stiffer ones, then further increasing of their stiffness may lead to the enlarging as well as to the diminishing of the absolute value of the stress intensity factor. The essential length scale of each periodic composite is the thickness of the repetitive cell. The influence of this parameter on the stress intensity factor was examined and found to be limited.

The composites considered in this paper are bi-material ones with the repetitive cell consisting of two isotropic elastic layers. The application of the method in the more complicated cases of anisotropic materials or increased number of layers in the cell seems to be the next logical step in the topic.

Acknowledgements

The authors would like to acknowledge the help of Professor Nuller. Professor Boris Nuller has passed away in September 2002.

Appendix A

$$\boldsymbol{M}=\begin{bmatrix}
\mu c_1 & -\mu s_1 & -\mu z_1 c_1 & \mu z_1 s_1 & -\gamma_m c_2 & -\gamma_m s_2 & -\gamma_m z_2 c_2 & -\gamma_m z_2 s_2 \\
\mu s_1 & \mu c_1 & -\mu d_1 & \mu e_1 & \gamma_m s_2 & -\gamma_m c_2 & \gamma_m d_2 & \gamma_m e_2 \\
-\hat{\mu} c_1 & \hat{\mu} s_1 & \hat{\mu} z_1 c_1 + \frac{\eta_1}{2} s_1 & \frac{\eta_1}{2} c_1 - \hat{\mu} z_1 s_1 & 0 & 0 & \frac{\gamma_m \eta_2}{2} s_2 & -\frac{\gamma_m \eta_2}{2} c_2 \\
\hat{\mu} s_1 & \hat{\mu} c_1 & -\hat{\mu} z_1 s_1 - \eta_3 c_1 & \eta_3 s_1 - \hat{\mu} z_1 c_1 & 0 & 0 & \frac{\gamma_m \eta_1}{2} c_2 & \frac{\gamma_m \eta_1}{2} s_2 \\
-\mu & 0 & 0 & 0 & 1 & 0 & 0 & 0 \\
0 & -\mu & \mu k_1 & 0 & 0 & 1 & -k_2 & 0 \\
-2 & 0 & 0 & -\eta_1 & 2 & 0 & 0 & \eta_2 \\
0 & 2 & -\zeta_1 & 0 & 0 & -2 & \zeta_2 & 0
\end{bmatrix},$$

where

$$z_i = h_i z, \quad c_i = \cos z_i, \quad s_i = \sin z_i,$$

$$\eta_i = \kappa_i + 1, \quad \zeta_i = \kappa_i - 1, \quad \eta_3 = \mu\kappa_1 - \zeta_1/2, \quad \hat{\mu} = \mu - 1,$$

$$d_i = \kappa_i c_i + z_i s_i, \quad e_i = \kappa_i s_i - z_i c_i, \quad i = 1, 2.$$

Appendix B

The elements of the matrix in (20) are presented on the imaginary axis $z = \mathrm{i}t$

$$s_{ij} = \frac{a_{ij}}{\det(\boldsymbol{M})},$$

where

$$\begin{aligned}\det(\boldsymbol{M}) = {} & \eta_4(\gamma_m^4 + 1) + 4\eta_4(\hat{\mu}(\lambda_0 - 2h_1h_2\hat{\mu}t^2)C_3 - \lambda_{12}C_4)g_1\gamma_m \\ & - (4\lambda_{12}\lambda_0(C_2 + C_1)\hat{\mu} - 2\lambda_{12}^2C_6 - 2\hat{\mu}^2\lambda_0^2C_5 - 4(\lambda_0\hat{\mu} + (\kappa_2\kappa_1 + 1)\mu)(\mu^2\kappa_1 + \kappa_2) \\ & - 4\mu^2((\kappa_2^2 + \eta_2)(\kappa_1^2 + \eta_1) + 3\kappa_2\kappa_1) - 4t^2(4h_{12}^2t^2 + \lambda_7 - 2(h_1^2C_2\lambda_1^2 + h_2^2C_1\lambda_2^2)\hat{\mu}^2))\gamma_m^2,\end{aligned}$$

and

$$\begin{aligned}a_{11} = {} & \eta_4\gamma_m(2t\hat{\mu}((h_1\kappa_2 - h_2)\gamma_m^2 + \mu(h_1 - \kappa_1h_2))S_3 + 2t(\lambda_1h_1 + \lambda_2h_2)(\gamma_m^2 - \mu)S_4 - (n_2g_1 + 2\lambda_{12})C_4 \\ & - (4h_1h_2\hat{\mu}(\hat{\mu} - g_1)t^2 + n_3g_1 - 2\lambda_0\hat{\mu})C_3) + (2t\hat{\mu}\eta_4(\lambda_2h_2S_1 + h_1\lambda_1S_2) - 4\hat{\mu}(h_2^2\lambda_2\lambda_8C_1 + \lambda_1n_1h_1^2C_2)t^2 \\ & + (C_2 + C_1)(\lambda_1(\lambda_2^2 + \hat{\mu}\eta_2) + (-\hat{\mu}\kappa_2\lambda_0 + n_1\lambda_1)\lambda_2) + \lambda_{12}n_2C_6 - \lambda_0\hat{\mu}n_3C_5 - 16h_1^2h_2^2\hat{\mu}^3t^4 \\ & + 4\hat{\mu}(\lambda_1n_1h_1^2 - \eta_4h_1h_2(3 - \mu) + \lambda_2\lambda_8h_2^2)t^2 + 2\eta_4^2 - \eta_4\lambda_0 - \hat{\mu}(\kappa_2\lambda_2 - \lambda_0)(\lambda_1 - \lambda_0))\gamma_m^2 + \eta_4^2,\end{aligned}$$

$$\begin{aligned}a_{13} = {} & \mathrm{i}\eta_4\gamma_m((4h_1h_2\hat{\mu}(\gamma_m^2 + \mu)t^2 + \mu g_1(\kappa_2 - \kappa_1))S_3 - \mu g_1(\kappa_2\kappa_1 - 1)S_4 - 2t(\lambda_1h_1 + \lambda_2h_2)(\gamma_m^2 + \mu)C_4 \\ & - 2t\hat{\mu}((h_2 + h_1\kappa_2)\gamma_m^2 - \mu(\kappa_1h_2 + h_1))C_3) + \mathrm{i}\mu\gamma_m^2(\eta_1((4t^2h_2^2 - \kappa_2)\lambda_2\hat{\mu} + \lambda_1\lambda_0)S_1 \\ & - \eta_2((4t^2\lambda_1h_1^2 - \kappa_1)\lambda_1\hat{\mu} + \lambda_0\lambda_2)S_2 + \lambda_0\hat{\mu}(\kappa_2 - \kappa_1)S_5 + \lambda_{12}(\kappa_2\kappa_1 - 1)S_6 + 2t(\hat{\mu}h_1\zeta_2\lambda_1\eta_1C_2 \\ & - \hat{\mu}\eta_2\lambda_2\zeta_1h_2C_1 + 4h_{12}(\eta_1h_2 + h_1\eta_2)t^2 + \eta_5)),\end{aligned}$$

$$\begin{aligned}a_{21} = {} & -a_{13} + 4It\gamma_m(-\eta_4(\lambda_1h_1 + \lambda_2h_2)(\gamma_m^2 + \mu)C_4 - \eta_4\hat{\mu}((\kappa_2\gamma_m^2 - \mu)h_1 + (\gamma_m^2 - \mu\kappa_1)h_2)C_3 \\ & + \gamma_m\mu(\hat{\mu}h_1\zeta_2\lambda_1\eta_1C_2 - \hat{\mu}\eta_2\lambda_2\zeta_1h_2C_1 + 4h_{12}(\eta_1h_2 + h_1\eta_2)t^2 + \eta_5)),\end{aligned}$$

$$a_{23} = a_{11} - 4t\gamma_m\eta_4(\hat{\mu}((\mu + \kappa_2\gamma_m^2)h_1 - (\mu\kappa_1 + \gamma_m^2)h_2)S_3 + (\gamma_m^2 - \mu)(\lambda_1h_1 + \lambda_2h_2)S_4 + \hat{\mu}\gamma_m(\lambda_2h_2S_1 + h_1\lambda_1S_2))$$

with

$$g_1 = 1 + \gamma_m^2, \quad h_{12} = h_1h_2\hat{\mu}^2, \quad \eta_4 = \mu\eta_1\eta_2,$$

$$\lambda_0 = \mu\kappa_1 - \kappa_2, \quad \lambda_1 = \mu + \kappa_2, \quad \lambda_2 = \mu\kappa_1 + 1,$$

$$\lambda_7 = 2\hat{\mu}^2(\lambda_1^2h_1^2 + 2\eta_4h_2h_1 + \lambda_2^2h_2^2), \quad \lambda_8 = \hat{\mu} - \lambda_2, \quad \lambda_{12} = \lambda_1\lambda_2,$$

$$n_1 = \hat{\mu}\kappa_2 - \lambda_1, \quad n_2 = \kappa_2\lambda_2 + \lambda_1, \quad n_3 = \lambda_0 + \hat{\mu}\kappa_2, \quad C_1 = \cosh 2th_1,$$

$$C_2 = \cosh 2th_2, \quad C_3 = \cosh t(h_1 - h_2), \quad C_4 = \cosh th, \quad C_5 = \cosh 2t(h_1 - h_2),$$

$$C_6 = \cosh 2th, \quad S_1 = \sinh 2th_1, \quad S_2 = \sinh 2th_2, \quad S_3 = \sinh t(h_1 - h_2),$$

$$S_4 = \sinh th, \quad S_5 = \sinh 2t(h_1 - h_2), \quad S_6 = \sinh 2th,$$

$$\eta_5 = \eta_1(\mu\eta_2^2 + \lambda_1^2 - \hat{\mu}^2\kappa_2)h_1 + \eta_2(\mu\eta_1^2 + \lambda_2^2 - \hat{\mu}^2\kappa_1)h_2.$$

References

Babushka, I., Szabo, B.A., Actis, R.L., 1992. Hierarchy methods for laminated composites. International Journal for Numerical Methods in Engineering 33 (3), 503–535.

Bruno, D., Greco, F., 2001. Mixed mode delamination in plates: are fined approach. International Journal of Solids and Structures 38, 9149–9177.

Carrera, E., Demasi, L., 2002. Classical and advanced multilayered plate elements based upon PVD and RVMT. Part I: Derivation of finite element matrices. International Journal for Numerical Methods in Engineering 55 (2), 191–231.

Charalambides, P.G., 1991. Steady-state mechanics of delamination cracking in laminated ceramic–matrix composites. Journal of American Ceramics Society 74, 3066–3080.

Chatterjee, S.N., 1987. Three- and two-dimensional stress fields near delaminations in laminated composite plates. International Journal of Solids and Structures 23 (11), 1535–1549.

Dyskin, A.V., Germanovich, L.N., Ustinov, K.V., 2000. Asymptotic analysis of crack interaction with free boundary. International Journal of Solids and Structures 37, 857–886.

Erdogan, F., Gupta, G., 1971a. The stress analysis of multi-layered composites with a flaw. International Journal of Solids and Structures 7, 39–61.

Erdogan, F., Gupta, G., 1971b. Layered composites with an interface flaw. International Journal of Solids and Structures 7, 1089–1107.

Kaczyński, A., Matysiak, S.J., Pauk, V.I., 1994. Griffith crack in a laminated elastic layer. International Journal of Fracture 67, R81–R86.

Kamysheva, G.A., Nuller, B.M., Ryvkin, M.B., 1982. Deformation of an elastic plane reinforced by a periodic system of non-periodically loaded oblique semi-infinite stringers. Mechanics of Solids 17 (3), 104–109.

Karpov, E.G., Dorofeev, D.L., Stephen, N.G., 2002. On static analysis of finite repetitive structures by discrete Fourier transform. International Journal of Solids and Structures 39 (16), 4291–4310.

Kucherov, L., Ryvkin, M., 2002. Interface crack in periodically layered bimaterial composite. International Journal of Fracture 117, 175–194.

Malishev, B.M., Salganik, R.L., 1965. The strength of adhesive joints using the theory of crack. International Journal of Fracture Mechanics 1, 114–128.

Nuller, B., 1981. On the elastic deformation of a layered plate and a half-space. Proceedings of the All-Union Research Institute of Hydraulic Engineering (VNIIG) 151, 25–30 (in Russian).

Nuller, B., Ryvkin, M., 1980. On the boundary value problems for elastic domains of the periodical structure deformed by arbitrary loads. Proceedings of the All-Union Research Institute of Hydraulic Engineering (VNIIG) 136, 49–55 (in Russian).

Pagano, N.J., 1969. Exact solutions for composite laminates in cylindrical bending. Journal of Composite Materials 3, 398–411.

Pagano, N.J., 1970. Exact solutions for rectangular bi-direction composites and sandwich plates. Journal of Composite Materials 4, 20–34.

Rice, J.R., 1988. Elastic fracture mechanics concepts for interfacial cracks. Journal of Applied Mechanics 55, 98–103.

Rice, J.R., Sih, G.C., 1965. Plane problems of cracks in dissimilar media. Journal of Applied Mechanics 32, 418–423.

Ryvkin, M., Nuller, B., 1997. Solution of quasi-periodic fracture problems by representative cell method. Computational Mechanics 20, 145–149.

Ryvkin, M., Kucherov, L., 2001. An inverse shielding effect in a periodically layered composite. International Journal of Fracture 108, L3–L8.

Schoeppner, G.A., Pagano, N.J., 1998. Stress fields and energy release rates in cross-ply laminates. International Journal of Solids and Structures 35 (11), 1025–1055.

Sheinman, I., Kardomates, G.A., 1997. Energy release rates and stress intensity factors for delaminated composite laminates. International Journal of Solids and Structures 34 (4), 451–459.

Uflyand, I.S., 1968. Integral transforms in problems of the theory of elasticity. Nauka, Leningrad (in Russian).